ACS APPLIED MATERIALS & INTERFACES

Letter

www.acsami.org

Mercury Ion Responsive Wettability and Oil/Water Separation

Liangxin Xu, Na Liu, Yingze Cao, Fei Lu, Yuning Chen, Xiaoyong Zhang, Lin Feng,* and Yen Wei

Department of Chemistry, Tsinghua University, Beijing 100084, P. R. China

Supporting Information

ABSTRACT: A novel Hg^{2+} responsive oil/water separation mesh with poly(acrylic acid) hydrogel coating is reported. The mesh can separate oil and water because of the superhydrophilicity of the poly(acrylic acid) hydrogel coating on the mesh, and switch the wettability based on the chelation between Hg^{2+} and poly(acrylic acid) . The reversible change in oil contact angle of as-prepared mesh is about 149° after immersion in Hg^{2+} solution. This mesh is an ideal candidate for oil-polluted water purification, especially for water that contains Hg^{2+} contaminant.

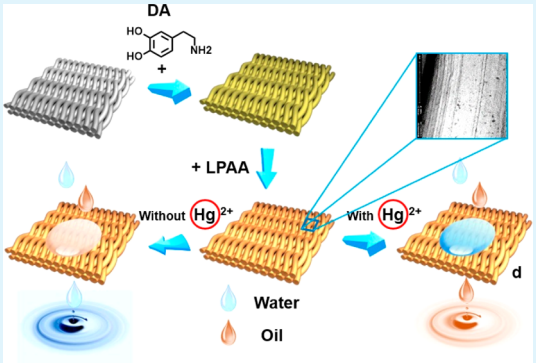

KEYWORDS: *mercury ion, response, wettability, oil/water separation*

On October 10, 2013, a global effort to address mercury (Hg) was the addressed at the Minamata Convention on Mercury.[1−4] Hg is a notorious heavy metal with significant health and environmental effects.[5,6] Hg and its various compounds lead to a wide range of serious health problems including brain and neurological damage, particularly among the young.[7,8] Polluted water is the main carrier of anthropogenic mercury contaminants, which generally contains insoluble oil and other soluble pollutants during the global industrial production.[9,10] Therefore, several strategies, including mercury contaminant detection and oil/water separation, are in demand for sewage treatment. Accordingly, a novel material that could not only selectively detect Hg^{2+} but also effectively separate the mixtures of oil and water will be a wise choice for future industrial wastewater treatment.

Hg^{2+} is an excellent chelate metal ion, and a large sum of sensors can effectively detect Hg^{2+} with fluorescence or color changes based on chelation.[11] For example, rhodamine,[12] naphthalimide,[13] 4,4-difluoro-4-bora-3a, 4a-diaza-s-indancene (BODIPY),[14] anthracene,[15] acridine,[16] porphyrin,[17] β-cyclodextrin,[18] thymine-rich DNA,[19−23] nanoparticles,[24] and their derivatives are common functional groups on sensors. However, studies with mercury mainly concentrate on fluorescent, colorimetric detection and cold vapor atomic adsorption spectrometry; there are few studies on the other areas of mercury.

To date, the majority of Hg^{2+} detection and oil/water separation have been performed separately. Our group made efforts to the wettability of material, including superhydrophobic and superoleophilic polytetrafluoroethylene (PTFE) coated mesh,[25] photoresponsive and photodegradable TiO_2-based mesh[26] and et al.[27−29] Recently, we developed a polyacrylamide hydrogel-coated mesh, and the superhydrophilicity of this mesh makes it an outstanding oil/water separation material.[30,31] It is known that poly(acrylic acid) is a hydrophilic material and can chelate many metal ions including mercury. Herein, we have developed a new material for industrial wastewater treatment via combining polydopamine coated mesh (PDA mesh) with linear poly(acrylic acid) (LPAA), which can separate oil and water because of the hydrophilicity of LPAA, and switch the wettability of the mesh based on chelation between mercury and LPAA (Scheme 1). This novel mesh is hydrophilic and oleophobic in the absence of Hg^{2+} ($Hg(NO_3)_2$, mercuric nitrate, 40.48 mg/mL), resulting in that water can permeate through the mesh while oil is blocked (Scheme 1d). However, the mesh changes to oleophilic and hydrophobic in the presence of Hg^{2+} to make that oil can go through the mesh whereas water is obstructed (Scheme 1d′). Such kind of mesh is an ideal candidate for oil-polluted water purification, especially that contains Hg^{2+} contaminant.

Scheme 1a−c illustrate the fabrication of LPAA-PDA mesh. First, PDA mesh is manufactured by dopamine self-polymerization on the surface of stainless steel mesh in Tris solution (10 mmol/L, pH 8.5, Scheme 1b, see the experimental details in the Supporting Information).[32−34] PDA mesh possesses high reaction activity with thiol and amino groups due to the unsaturated ketone groups of polydopamine (PDA).[35,36] In NaOH solution (pH >12), thiol groups are obtained from the hydrolysis of chain transfer agent (CTA, Scheme 2), which is the active chain end of reversible addition−fragmentation chain transfer (RAFT) polymerized LPAA chain. Then, LPAA-PDA mesh is obtained via Michael reaction between the thiol group of LPAA and the unsaturated ketone group of PDA in NaOH solution (pH >12), followed by the hydrolysis (Scheme 1c).

Received: June 16, 2014
Accepted: August 11, 2014
Published: August 11, 2014

Scheme 1. Diagram of Preparation, Oil/Water Separation, and Wettability Transition of Mussel-Inspired Hydrogel Coated Mesh: (a) Stainless Steel Mesh; (b) Polydopamine-Coated Mesh (PDA mesh); (c) Linear Polyacrylic Acid Grafted to PDA Mesh (LPAA-PDA mesh); (d) Oleophilic and Hydrophobic Properties of LPAA-PDA Mesh in the Presence of Hg^{2+}; (d′) Hydrophilic and Oleophobic Properties of LPAA-PDA Mesh in the Absence of Hg^{2+}

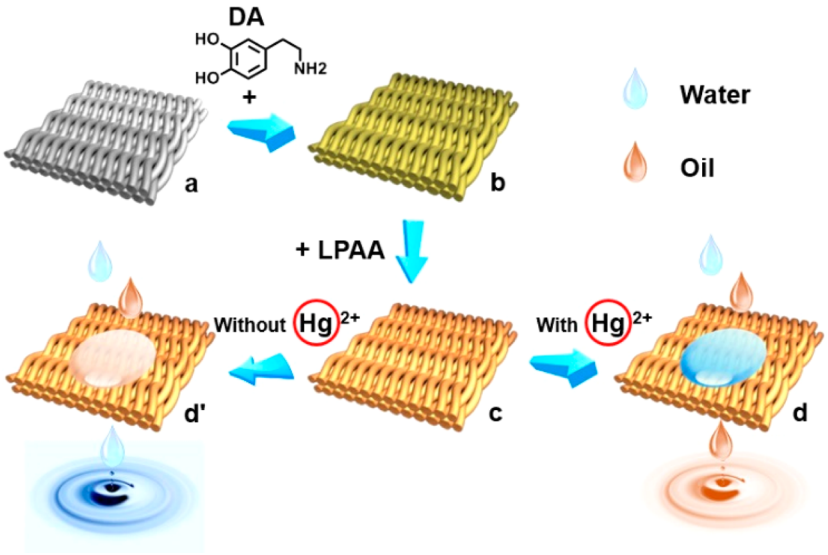

The scanning electron microscope (SEM) images of the original stainless steel mesh, PDA mesh, LPAA-PDA mesh and LPAA-PDA mesh after immersed in saturated Hg^{2+} solution are shown in Figure 1. Stainless steel mesh with 1000 mesh size is chosen as a substrate because stainless steel owns high compressive strength and is not readily corroded, rusted, or stained with water compared to ordinary steel. Figure 1a illustrates the smooth surface of stainless steel with a diameter about 50 μm, while "island shape" polymers (red circle) appear on the surface after PDA conjugates to the stainless steel mesh (Figure 1b). Similarly, there are "island shape" polymer mixtures on the surface of LPAA-PDA mesh and LPAA-PDA mesh after immersed in saturated Hg^{2+} solution (Figure 1c, d).

Surface constituent elements of each meshes have been measured by X-ray photoelectron spectroscopy (XPS), which can reflect the chemical modification of the mesh and the chelation between Hg^{2+} and poly(acrylic acid) . Figure 2a elucidates three essential elements including nitrogen (N), carbon (C) and mercury (Hg) on the spectra that were surveyed by scanning binding energy from 0 to 500 eV. The three main peaks at 399.8, 284.8, and 105.8 eV were respectively labeled as N 1s, C 1s and Hg 4f5 (Figure 2a). In Figure 2b, the peak at 399.8 eV originates from sp3-hybridized nitrogen atoms. Compared to original stainless steel mesh, N content of PDA mesh increases, implying the conjugation of polydopamine to mesh. Similarly, it indicates the intensity enhancement of C 1s peak to contrast LPAA-PDA mesh with PDA mesh in Figure 2c, because the LPAA contains carbon, whereas LPAA was grafted to the PDA mesh via Michael addition reaction.[36] Furthermore, the strong Hg 4f5 peak was observed at 105.8 eV binding energy in Figure 2d after LPAA-PDA mesh immerses in saturated Hg^{2+} solution, suggesting that the chelation between Hg^{2+} and poly(acrylic acid) produce mercury polyacrylate.

To characterize the surface wettability transition of as-prepared meshes, the water contact angle in the air (WCA) and oil contact angle under the water (OCA) of each mesh has been determined. Figure 3 displays the morphologies of water droplets in air and oil droplets under water on these meshes. It is observed that the WCA of original stainless steel mesh is

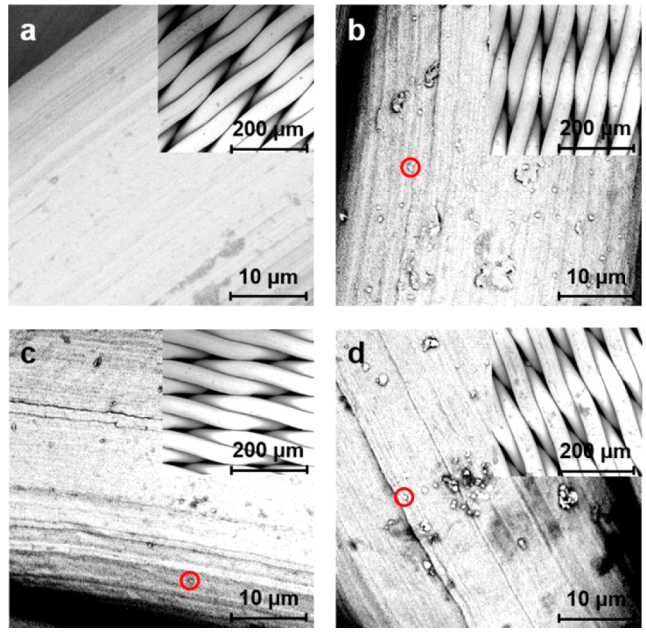

Figure 1. SEM images of the as-prepared mesh: (a) Stainless steel mesh. (b) Polydopamine-coated mesh (PDA mesh). (c) Linear poly(acrylic acid) grafted to PDA mesh (LPAA-PDA mesh). (d) LPAA-PDA mesh after immersion in saturated Hg^{2+} solution.

131.9 ± 1.1°, and the OCA is 129.3 ± 3.2° (Figure 3A). As stainless steel mesh is modified by PDA, the WCA decreases to 67.0 ± 5.8° and the OCA increases to 143.5 ± 2.5° to make this PDA mesh a highly oleophobic mesh (Figure 3B). After hydrophilic LPAA was grafted to PDA via Michael addition reaction, the LAPP-PDA mesh becomes a superhydrophilic (0°) and highly oleophobic (149.0 ± 2.4°) mesh while the water droplet can quickly spread this mesh (Figure 3C). Next, the hydrophilic LPAA-PDA mesh converts to hydrophobic mesh that the WCA of LPAA-PDA meshes increase from 0° to 121.9 ± 3.4°,to 121.4 ± 2.7° (Figure 3C–E), because the complexation between poly(acrylic acid) and Hg^{2+} induces the

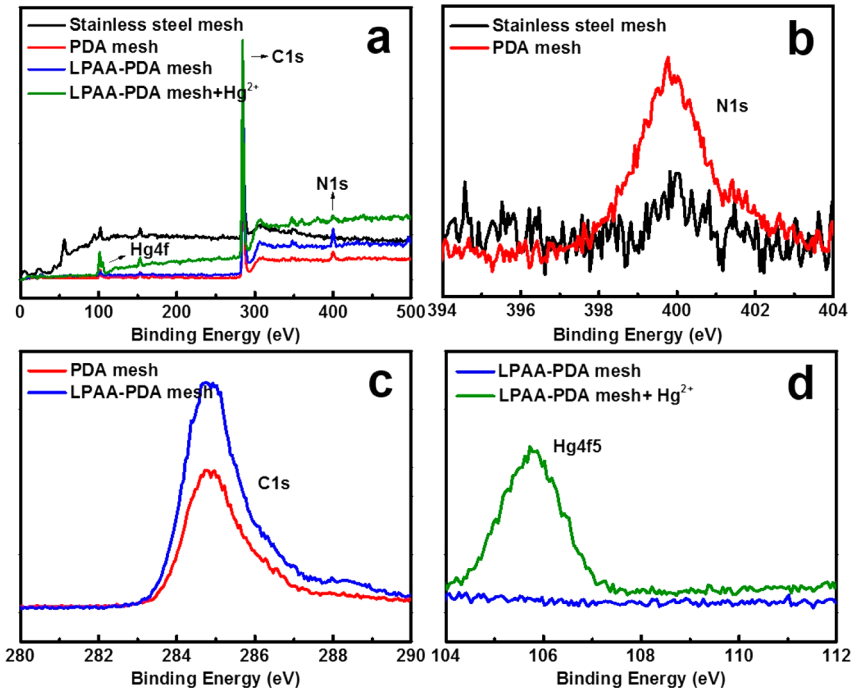

Figure 2. XPS spectra of the as-prepared mesh: (a) Survey scans the spectral region from 0 to 500 eV. (b–d) high-resolution XPS N 1s, C 1s, and Hg 4f5 narrow scans as a function of electron binding energy. (b) Content of N increases after dopamine self-polymerization on stainless steel mesh. (c) Conjugation of LPAA and PDA mesh leads to the increase of C content. (d) Mercury element is observed after LPAA-PDA mesh immersion in saturated Hg^{2+} solution.

No.	**A.** Stainless Steel Mesh	**B.** PDA Mesh	**C.** PLAA-PDA Mesh	**D.** 1 mg/mL Hg^{2+} Solution	**E.** Saturated Hg^{2+} Solution
Water Contact Angle in the Air	131.9±1.1 °	67.0±5.8 °	0 °	121.9±3.4 °	121.4±2.7 °
Oil Contact Angle in the Water	129.3±3.2 °	143.5±2.5 °	149.0±2.4 °	138.1±4.1 °	0 °

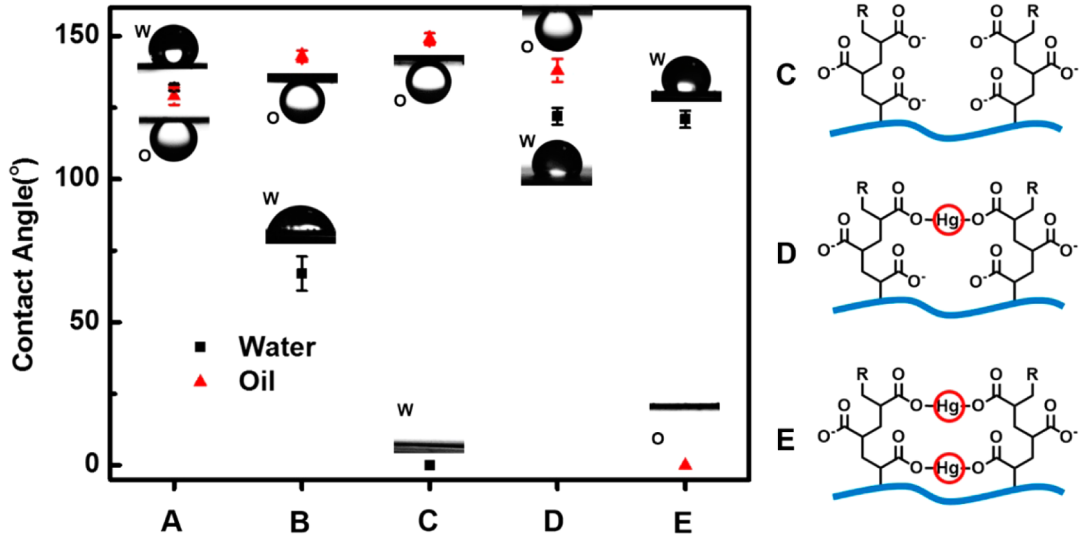

Figure 3. Contact angle images illustrate the wettability transition of as-prepare meshes: (A) Hydrophobic and underwater oleophobic stainless steel mesh. (B) Underwater highly oleophobic PDA mesh. (C) Superhydrophilic and underwater oleophobic LPAA-PDA mesh. (D) Hydrophobic and under water oleophobic LPAA-PDA mesh after soaking in 1 mg/mL Hg^{2+} solution for 5 min. (E) Hydrophobic and under water oleophilic LPAA-PDA mesh after soaking in a saturated Hg^{2+} solution for 5 min. Hg^{2+} results in wettability transition of LPAA-PDA mesh due to the chelation between Hg^{2+} and poly(acrylic acid) . W, water contact angle; O, oil contact angle.

anionic poly(acrylic acid) change to neutral mercury polyacrylate (Figure 3D, E).[37] Consequently, the oil contact angle of LPAA-PDA meshes demonstrates that the as-prepared meshes are oleophobic except the LPAA-PDA mesh immersed

Scheme 2. Reversible Addition−Fragmentation Chain Transfer (RAFT) Polymerization and Hydrolysis of Linear Polyacrylic Acid (LPAA)

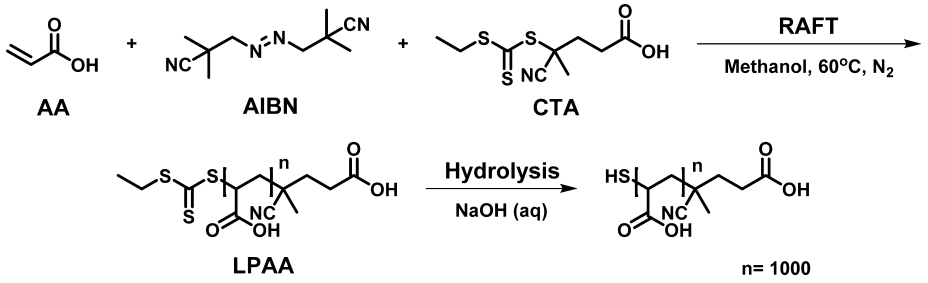

in saturated Hg^{2+} solution (Figure 3C−E). With increasing of the Hg^{2+} concentration, the meshes turn to more oleophilic from 149.0 ± 2.4°, to 138.1 ± 4.1° to 0°, because of the generation of more neutarl mercury polyacrylate. The concentration of Hg^{2+} is so high in saturated Hg^{2+} solution that generates plenty of neutral mercury polyacrylate to achieve wettability transition of LPAA-PDA mesh. Therefore, the mechanism for Hg^{2+}-induced wettability of LPAA-PDA meshes is caused by the polarity varition of LPAA. LPAA is polar and negative while mercury polyacrylate is nonpolar and neutral after LPAA-PDA meshes soaking in a saturated Hg^{2+} solution. And this transition process might relate to the conformation change of LPAA chains in the presence of mercury ions. Besides, Na^{+}, Ca^{2+}, Ni^{2+}, and Cd^{2+} are tested as responsive ions, but the WCA data do not show a change (see the Supporting Information, Figure S2).The difference is caused by the polarity of sodium polyacrylate and calcium polyacrylate but the nonpolarity of mercury polyacrylate.

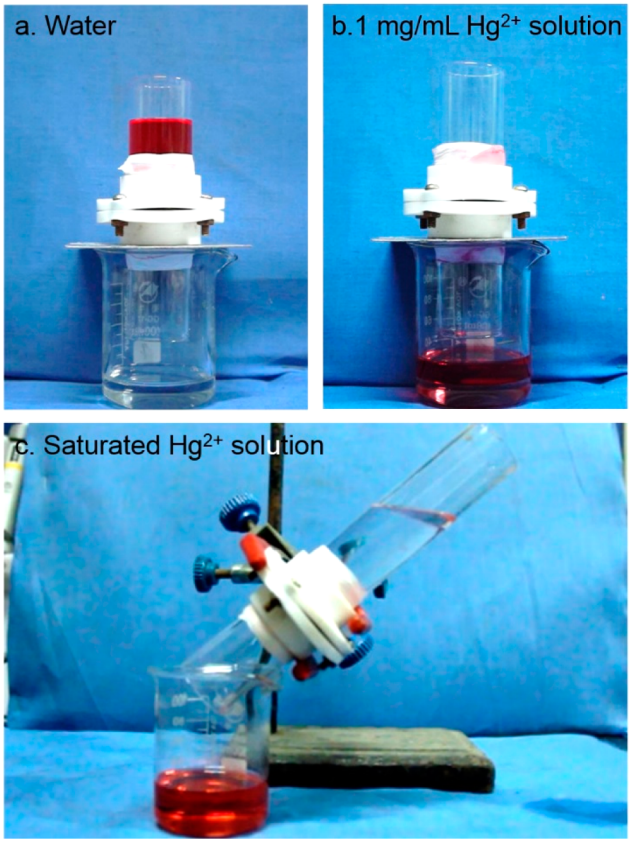

Figure 4. Oil/water separation studies of LPAA-PDA meshes. (a) LPAA-PDA mesh,. (b) LPAA-PDA mesh after soaking in 1 mg/mL Hg^{2+} solution, (c) LPAA-PDA mesh after soaking in a saturated Hg^{2+} solution. Red, petroleum ether with oil red; colorless, water.

The Hg^{2+} responsive wettability transition of LPAA-PDA mesh implies that this mesh can be utilized to oil/water separation under the conditions of different Hg^{2+} concentration. A series of studies to separate oil and water were performed as showed in Figure 4. LPAA-PDA mesh was fixed between two glass tubes. Mixtures of petroleum ether (dyed by oil red) and water (50% v/v) were poured onto the LPAA-PDA mesh. Water quickly permeated through the mesh and dropped into the beaker below (Figure 4a, see the Supporting Information, Movie S1). Meanwhile, oil was retained above the mesh because of the underwater superoleophobic and low oil-adhesion properties of the poly(acrylic acid) hydrogel. No external force but their own weight was employed during the separation process, which indicates this water-removing hydrogel-coated mesh is a good candidate in industrial oil-polluted water treatments and oil spill cleanup. After soaking in 1 mg/mL Hg^{2+} solution and dried, both water and oil can go through the meshes because that the poly(acrylic acid) hydrogel has been destroyed by the generated neutral mercury polyacrylate (see Figure 4b that Supporting Information, Movie S2). When enough mercury polyacrylate replaces poly(acrylic acid), the hydrophilic hydrogel-coated mesh turns oleophilic, and oil can readily permeate through the mesh (Figure 4c, see the Supporting Information, Movie S3).

CONCLUSIONS

We successfully developed a new method to achieve wettability response to Hg^{2+} with a linear poly(acrylic acid) hydrogel. This novel mesh achieves effectively oil/water separation on account of the hydrophilicity of linear poly(acrylic acid) , and switches the wettability of the mesh based on chelation between mercury and poly(acrylic acid) , which makes it a good candidate in industrial oil-polluted water treatments and oil spill cleanup. In the future, more heavy metal ions, such as Pb^{2+}, Cr^{3+}, Ag^{+}, Au^{3+}, etc., will have ideal wettability response factors besides light, temperature, pH, electric field, and pressure. The applied research including oil/water separation, emulsion separation, stability, and reusability of ion-induced wettability will be a new research area.

ASSOCIATED CONTENT

Supporting Information

Material and characterization; experimental details of LPAA-PDA mesh; contact angle of LPAA-PDA meshes after soaking in saturated Na^{+}, Ca^{2+}, Ni^{2+}, Cd^{2+}, and Hg^{2+}; and oil/water separation videos of the as-prepared mesh, etc. This material is available free of charge via the Internet at http://pubs.acs.org/.

AUTHOR INFORMATION

Corresponding Author

*E-mail: fl@mail.tsinghua.edu.cn.

Funding

National Natural Science Foundation (51173099, 21134004), National High Technology Research and Development Program of China (2012AA030306), National Research Fund for Fundamental Key Projects (2011CB935700).

Notes

The authors declare no competing financial interest.

ACKNOWLEDGMENTS

The authors are grateful for financial support from the National Natural Science Foundation (51173099, 21134004), the National High Technology Research and Development Program of China (2012AA030306), and the National Research Fund for Fundamental Key Projects (2011CB935700).

ABBREVIATIONS

Hg, mercury
BODIPY, 4, 4-difluoro-4-bora-3a, 4a-diaza-s-indancene
PTFE, polytetrafluoroethylene
PDA, polydopamine
PDA mesh, polydopamine coated mesh
LPAA, linear poly(acrylic acid)
LPAA-PDA mesh, linear poly(acrylic acid) grafted to PDA mesh
CTA, chain transfer agent
RAFT, reversible addition−fragmentation chain transfer
SEM, scanning electron microscope
XPS, X-ray photoelectron spectroscopy
WCA, water contact angle in the air
OCA, oil contact angle under the water
AA, acrylic acid

REFERENCES

(1) Kessler, R. the Minamata Convention on Mercury: A First Step toward Protecting Future Generations. *Environ. Health Perspect.* **2013**, *121*, A304−A309.

(2) Lubick, N.; Malakoff, D. With Pact's Completion, the Real Work Begins. *Science* **2013**, *341*, 1443−1445.

(3) Normile, D. Mercury Pollution In Minamata, Mercury Still Divides. *Science* **2013**, *341*, 1446−1447.

(4) Wade, L. Mercury Pollution Gold's Dark Side. *Science* **2013**, *341*, 1448−1449.

(5) Bolger, P. M.; Schwetz, B. A. Mercury and Health. *N. Engl. J. Med.* **2002**, *347*, 1735−1736.

(6) Pirrone, N.; Cinnirella, S.; Feng, X.; Finkelman, R. B.; Friedli, H. R.; Leaner, J.; Mason, R.; Mukherjee, A. B.; Stracher, G. B.; Streets, D. G.; Telmer, K. Global Mercury Emissions to the Atmosphere from Anthropogenic and Natural Sources. *Atmos. Chem. Phys.* **2010**, *10*, 5951−5964.

(7) Mozaffarian, D.; Shi, P.; Morris, J. S.; Spiegelman, D.; Grandjean, P.; Siscovick, D. S.; Willett, W. C.; Rimm, E. B. Mercury Exposure and Risk of Cardiovascular Disease in Two U.S. Cohorts. *N. Engl. J. Med.* **2011**, *364*, 1116−1125.

(8) Mozaffarian, D.; Shi, P. L.; Morris, J. S.; Grandjean, P.; Siscovick, D. S.; Spiegelman, D.; Hu, F. B. Methylmercury Exposure and Incident Diabetes in US Men and Women in Two Prospective Cohorts. *Diabetes Care* **2013**, *36*, 3578−3584.

(9) Pacyna, E. G.; Pacyna, J. M.; Steenhuisen, F.; Wilson, S. Global Anthropogenic Mercury Emission Inventory for 2000. *Atmos. Environ.* **2006**, *40*, 4048−4063.

(10) Pacyna, E. G.; Pacyna, J. M.; Sundseth, K.; Munthe, J.; Kindbom, K.; Wilson, S.; Steenhuisen, F.; Maxson, P. Global Emission of Mercury to the Atmosphere from Anthropogenic Sources in 2005 and Projections to 2020. *Atmos. Environ.* **2010**, *44*, 2487−2499.

(11) Kim, H. N.; Ren, W. X.; Kim, J. S.; Yoon, J. Fluorescent and Colorimetric Sensors for Detection of Lead, Cadmium, and Mercury Ions. *Chem. Soc. Rev.* **2012**, *41*, 3210−3244.

(12) Huang, W.; Zhu, X.; Wua, D. Y.; He, C.; Hu, X. Y.; Duan, C. Y. Structural Modification of Rhodamine-Based Sensors toward Highly Selective Mercury Detection in Mixed Organic/Aqueous Media. *Dalton Trans.* **2009**, 10457−10465.

(13) Fang, C. L.; Zhou, J.; Liu, X. J.; Cao, Z. H.; Shangguan, D. H. Mercury(II)-mediated Formation of Imide-Hg-imide Complexes. *Dalton Trans.* **2011**, *40*, 899−903.

(14) Atilgan, S.; Kutuk, I.; Ozdemir, T. A Near IR Di-styryl BODIPY-based Ratiometric Fluorescent Chemosensor for Hg(II). *Tetrahedron Lett.* **2010**, *51*, 892−894.

(15) Mitra, A.; Mittal, A. K.; Rao, C. P. Carbohydrate Assisted Fluorescence Turn-on Gluco-imino-anthracenyl Conjugate as a Hg(II) Sensor in Milk and Blood Serum Milieu. *Chem. Commun.* **2011**, *47*, 2565−2567.

(16) Lee, H. N.; Kim, H. N.; Swamy, K. M. K.; Park, M. S.; Kim, J.; Lee, H.; Lee, K. H.; Park, S.; Yoon, J. New Acridine Derivatives Bearing Immobilized Azacrown or Azathiacrown Ligand as Fluorescent Chemosensors for Hg(2+) and Cd(2+). *Tetrahedron Lett.* **2008**, *49*, 1261−1265.

(17) Yang, Y.; Jiang, J. H.; Shen, G. L.; Yu, R. Q. An Optical Sensor for Mercury Ion Based on the Fluorescence Quenching of Tetra(p-dimethylaminophenyl)porphyrin. *Anal. Chim. Acta* **2009**, *636*, 83−88.

(18) Fang, G.; Xu, M.; Zeng, F.; Wu, S. beta-Cyclodextrin as the Vehicle for Forming Ratiometric Mercury Ion Sensor Usable in Aqueous Media, Biological Fluids, and Live Cells. *Langmuir* **2010**, *26*, 17764−17771.

(19) Liu, X. F.; Tang, Y. L.; Wang, L. H.; Zhang, J.; Song, S. P.; Fan, C. H.; Wang, S. Optical Detection of Mercury(II) in Aqueous Solutions by Using Conjugated Polymers and Label-free Oligonucleotides. *Adv. Mater.* **2007**, *19*, 1471−1474.

(20) Li, T.; Dong, S. J.; Wang, E. Label-Free Colorimetric Detection of Aqueous Mercury Ion (Hg2+) Using Hg2+-Modulated G-Quadruplex-Based DNAzymes. *Anal. Chem.* **2009**, *81*, 2144−2149.

(21) Liu, C. W.; Huang, C. C.; Chang, H. T. Highly Selective DNA-Based Sensor for Lead(II) and Mercury(II) Ions. *Anal. Chem.* **2009**, *81*, 2383−2387.

(22) Zhang, L.; Tao, L.; Li, B.; Jing, L.; Wang, E. Carbon nanotube-DNA hybrid fluorescent sensor for sensitive and selective detection of mercury(II) ion. *Chem. Commun.* **2010**, *46*, 1476−1478.

(23) Dave, N.; Chan, M. Y.; Huang, P. J. J.; Smith, B. D.; Liu, J. W. Regenerable DNA-Functionalized Hydrogels for Ultrasensitive, Instrument-Free Mercury(II) Detection and Removal in Water. *J. Am. Chem. Soc.* **2010**, *132*, 12668−12673.

(24) Lin, C. Y.; Yu, C. J.; Lin, Y. H.; Tseng, W. L. Colorimetric Sensing of Silver(I) and Mercury(II) Ions Based on an Assembly of Tween 20-Stabilized Gold Nanoparticles. *Anal. Chem.* **2010**, *82*, 6830−6837.

(25) Feng, L.; Zhang, Z.; Mai, Z.; Ma, Y.; Liu, B.; Jiang, L.; Zhu, D. A Super-hydrophobic and Super-oleophilic Coating Mesh Film for the Separation of Oil and Water. *Angew. Chem., Int. Ed.* **2004**, *43*, 2012−2014.

(26) Gao, C. R.; Sun, Z. X.; Li, K.; Chen, Y. N.; Cao, Y. Z.; Zhang, S. Y.; Feng, L. Integrated Oil Separation and Water Purification by a Double-layer TiO2-based Mesh. *Energy Environ. Sci.* **2013**, *6*, 1147−1151.

(27) Xu, L. X.; Zhang, X. Y.; Zhu, C. Y.; Zhang, Y. L.; Fu, C. K.; Yang, B.; Tao, L.; Wei, Y. Nonionic Polymer Cross-linked Chitosan Hydrogel: Preparation and Bioevaluation. *J. Biomater. Sci., Polym. Ed.* **2013**, *24*, 1564−1574.

(28) Zhang, Y. L.; Yang, B.; Xu, L. X.; Zhang, X. Y.; Tao, L.; Wei, Y. Self-healing Hydrogels Based on Dynamic Chemistry and Their Biomedical Applications. *Acta Chim. Sin.* **2013**, *71*, 485−492.

(29) Xu, L. P.; Zhao, J.; Su, B.; Liu, X. L.; Peng, J. T.; Liu, Y. B. A.; Liu, H. L.; Yang, G.; Jiang, L.; Wen, Y. Q.; Zhang, X. J.; Wang, S. T. An Ion-Induced Low-Oil-Adhesion Organic/Inorganic Hybrid Film for Stable Superoleophobicity in Seawater. *Adv. Mater.* **2013**, *25*, 606−611.
(30) Xue, Z. X.; Wang, S. T.; Lin, L.; Chen, L.; Liu, M. J.; Feng, L.; Jiang, L. A Novel Superhydrophilic and Underwater Superoleophobic Hydrogel-Coated Mesh for Oil/Water Separation. *Adv. Mater.* **2011**, *23*, 4270−4273.
(31) Zhang, Y. L.; Yang, B.; Zhang, X. Y.; Xu, L. X.; Tao, L.; Li, S. X.; Wei, Y. A Magnetic Self-healing Hydrogel. *Chem. Commun.* **2012**, *48*, 9305−9307.
(32) Lee, H.; Dellatore, S. M.; Miller, W. M.; Messersmith, P. B. Mussel-inspired Surface Chemistry for Multifunctional Coatings. *Science* **2007**, *318*, 426−430.
(33) Zhang, X. Y.; Wang, S. Q.; Xu, L. X.; Feng, L.; Ji, Y.; Tao, L.; Li, S. X.; Wei, Y. Biocompatible Polydopamine Fluorescent Organic Nanoparticles: Facile Preparation and Cell Imaging. *Nanoscale* **2012**, *4*, 5581−5584.
(34) Qi, H. X.; Liu, M. Y.; Xu, L. X.; Feng, L.; Tao, L.; Ji, Y.; Zhang, X. Y.; Wei, Y. Biocompatibility Evaluation of Aniline Oligomers with Different End-functional Groups. *Toxicol. Res.* **2013**, *2*, 427−433.
(35) Xu, L. X.; Zhu, Y. F.; Shen, J. B.; Shi, J. B.; Tong, B.; Zhi, J. G.; Dong, Y. P. Synthesis of Phosphaphenanthrene-containing 4-ethynylbenzonate Grafted Glycidyl Azide Polymers by Click Chemistry and Their Aggregation-induced Emission Enhancement Properties. *Acta Polym. Sin.* **2011**, 740−744.
(36) Zhang, X. Y.; Ji, J. Z.; Zhang, X. Q.; Yang, B.; Liu, M. Y.; Liu, W. Y.; Tao, L.; Chen, Y. W.; Wei, Y. Mussel Inspired Modification of Carbon Nanotubes using RAFT Derived Stimuli-Responsive Polymers. *RSC Adv.* **2013**, *3*, 21817−21823.
(37) Tao, Y.; Lin, Y.; Huang, Z.; Ren, J.; Qu, X. Poly(acrylic acid)-templated Silver Nanoclusters as a Platform for Dual Fluorometric Turn-on and Colorimetric Detection of Mercury (II) Ions. *Talanta* **2012**, 290−294.